Physics in Medicine & Biology

IPEM Institute of Physics and Engineering in Medicine

PAPER

Detailed dosimetric evaluation of inter-fraction and respiratory motion in lung stereotactic body radiation therapy based on daily 4D cone beam CT images

To cite this article: Carlos Huesa-Berral *et al* 2023 *Phys. Med. Biol.* **68** 015005

View the article online for updates and enhancements.

You may also like

- Non-local total-variation (NLTV) minimization combined with reweighted L1-norm for compressed sensing CT reconstruction
Hojin Kim, Josephine Chen, Adam Wang et al.
- Automatic quantification of multi-modal rigid registration accuracy using feature detectors
F Hauler, H Furtado, M Jurisic et al.
- CT to cone-beam CT deformable registration with simultaneous intensity correction
Xin Zhen, Xuejun Gu, Hao Yan et al.

This content was downloaded from IP address 132.183.13.60 on 20/12/2022 at 16:55

IOP Publishing Phys. Med. Biol. 68 (2023) 015005 https://doi.org/10.1088/1361-6560/aca94d

Physics in Medicine & Biology

IPEM Institute of Physics and Engineering in Medicine

PAPER

RECEIVED
26 July 2022

REVISED
3 November 2022

ACCEPTED FOR PUBLICATION
6 December 2022

PUBLISHED
20 December 2022

Detailed dosimetric evaluation of inter-fraction and respiratory motion in lung stereotactic body radiation therapy based on daily 4D cone beam CT images

Carlos Huesa-Berral[1,2,3], Celia Juan-Cruz[1], Simon van Kranen[1], Maddalena Rossi[1], José Belderbos[1], Juan Diego Azcona[3], Javier Burguete[2] and Jan-Jakob Sonke[1,*]

[1] Department of Radiation Oncology, The Netherlands Cancer Institute, Plesmanlaan 121, 1066 CX Amsterdam, The Netherlands
[2] Physics and Applied Mathematics, School of Science, University of Navarra, E-31008 Pamplona, Navarra, Spain
[3] Service of Radiation Physics and Radiation Protection, University of Navarra Clinic, E-31008 Pamplona, Navarra, Spain
[*] Author to whom any correspondence should be addressed.

E-mail: j.sonke@nki.nl

Keywords: respiratory motion, inter-fractional anatomical variations, deformable image registration, daily dose calculation, 4D-CBCT

Supplementary material for this article is available online

Abstract

Objective. Periodic respiratory motion and inter-fraction variations are sources of geometric uncertainty in stereotactic body radiation therapy (SBRT) of pulmonary lesions. This study extensively evaluates and validates the separate and combined dosimetric effect of both factors using 4D-CT and daily 4D-cone beam CT (CBCT) dose accumulation scenarios. *Approach*. A first cohort of twenty early stage or metastatic disease lung cancer patients were retrospectively selected to evaluate each scenario. The planned-dose ($3D_{Ref}$) was optimized on a 3D mid-position CT. To estimate the dosimetric impact of respiratory motion ($4D_{Ref}$), inter-fractional variations ($3D_{Acc}$) and the combined effect of both factors ($4D_{Acc}$), three dose accumulation scenarios based on 4D-CT, daily mid-cone beam CT (CBCT) position and 4D-CBCT were implemented via CT-CT/CT-CBCT deformable image registration (DIR) techniques. Each scenario was compared to $3D_{Ref.}$ A separate cohort of ten lung SBRT patients was selected to validate DIR techniques. The distance discordance metric (DDM) was implemented per voxel and per patient for tumor and organs at risk (OARs), and the dosimetric impact for CT-CBCT DIR geometric errors was calculated. *Main results.* Median and interquartile range (IQR) of the dose difference per voxel were 0.05/2.69 Gy and −0.12/2.68 Gy for $3D_{Acc} - 3D_{Ref}$ and $4D_{Acc} - 3D_{Ref}$. For $4D_{Ref} - 3D_{Ref}$ the IQR was considerably smaller −0.15/0.78 Gy. These findings were confirmed by dose volume histogram parameters calculated in tumor and OARs. For CT-CT/CT-CBCT DIR validation, DDM (95th percentile) was highest for heart (6.26 mm)/spinal cord (8.00 mm), and below 3 mm for tumor and the rest of OARs. The dosimetric impact of CT-CBCT DIR errors was below 2 Gy for tumor and OARs. *Significance*. The dosimetric impact of inter-fraction variations were shown to dominate those of periodic respiration in SBRT for pulmonary lesions. Therefore, treatment evaluation and dose-effect studies would benefit more from dose accumulation focusing on day-to-day changes then those that focus on respiratory motion.

1. Introduction

Stereotactic body radiation therapy (SBRT) of pulmonary lesions has been shown to safely and accurately deliver a high dose to the tumor in a few fractions while limiting dose levels to healthy tissue (Yang and Timmerman 2018). Nevertheless, geometrical uncertainties associated with lung SBRT such as periodic respiratory motion, inter-fraction motion (day-to-day anatomical variations such as baseline shifts) and intra-fraction motion (tumor/organs drift during treatment delivery) influence the accuracy of imaging, treatment

© 2022 Institute of Physics and Engineering in Medicine

planning and treatment delivery (Sonke and Belderbos 2010, Schwarz *et al* 2017, Yang and Timmerman 2018). In this context, safety margins are applied around the target to account for those uncertainties (Van Herk 2004). Then, minimization of geometrical uncertainties and associated safety margins reduce toxicity (Sonke and Belderbos 2010, Schwarz *et al* 2017, Yang and Timmerman 2018) and/or allow dose escalation.

To minimize the impact of inter-fraction motion in the margins, daily image-guided radiotherapy (IGRT) systems like cone beam computed tomography (CBCT) are widely used in clinical practice since they allow to align the daily tumor position with the planned position (Jaffray *et al* 2002, Sonke *et al* 2005). Motion management techniques such as abdominal compression (Schwarz *et al* 2017, Yang and Timmerman 2018), breath-hold (Sonke and Belderbos 2010, Schwarz *et al* 2017, Yang and Timmerman 2018), gating or tumor tracking (Van Herk 2007, Sonke and Belderbos 2010, Ehrbar *et al* 2017, Schwarz *et al* 2017, Yang and Timmerman 2018, Keall *et al* 2021) may additionally be implemented to minimize breathing related misalignments. To reduce intra-fraction uncertainties, short treatment times, the acquisition of intra-arc CBCTs (Rossi *et al* 2016) and tumor trailing (Sonke and Belderbos 2010, Keall *et al* 2021) can be considered. In short, margin reduction can be achieved by further reducing uncertainties at the cost of added complexity, patient comfort, extra machinery, staff and training. Even so, there will always be residual uncertainties that require margins. Intra-fraction motion is the geometric uncertainty with the least geometric contribution to the construction of the safety margin (Sonke and Belderbos 2010, Rossi *et al* 2016), whereas periodic respiratory motion and inter-fraction variations have a larger contribution (Sonke and Belderbos 2010).

Geometric uncertainties associated with lung SBRT are well studied and there are different approaches to include them in the safety margins (Sonke and Belderbos 2010, Schwarz *et al* 2017, Yang and Timmerman 2018). Further studies regarding the dosimetric consequences of these geometric uncertainties, however, are necessary as they are less known (Brown *et al* 2021). Recently, Karlsson *et al* (2021) estimated the delivered dose to the target by simulating inter-fraction and breathing motion in SBRT and observed that breathing motion had a minor dosimetric impact compared to inter-fraction motion. This conclusion is widely accepted in clinical practice but is insufficiently evidenced (Brown *et al* 2021). However, as Karlsson *et al* (2021) pointed out, more accurate methodologies to evidence this are required for lung tumors, since a limitation in their study was the dose-shift invariance approximation they used to estimate the delivered dose: the static treatment planning dose matrix was shifted according to the simulations of setup, matching and breathing errors. For lung tumors, the dose-shift invariance assumption is a limitation, due to density changes and anatomical deformations. Moreover, such approach is limited to the dosimetric evaluation of the target and cannot analyze delivered dose to the surrounding normal tissue. In fact, the development of robust and validated methodologies to evaluate the treatment against respiratory motion and day-to-day anatomical variations remains a challenge (Giacometti *et al* 2018, 2020, Brown, *et al* 2021, Karlsson *et al* 2021)

The effect of periodic respiration and inter-fraction motion in the dose calculation process have been studied separately in more detail: recalculation of the dose at different 4D-CT phases and accumulation by using deformable image registration (DIR) has been validated to include respiration (Admiraal *et al* 2008, Mexner *et al* 2009, Valdes *et al* 2017, Azcona *et al* 2019), as well as strategies based on daily dose calculation in daily imaging (by the creation of virtual CT (vCT) (Giacometti *et al* 2018), Cole *et al* 2018, Yuan *et al* 2020, Szeto *et al* 2016) and mapping the daily dose for accumulation (Veiga *et al* 2015, Szeto *et al* 2016, Wang *et al* 2020) (by using DIR) for including inter-fraction motion. However, the lack of an objective metric to assess the DIR quality in CBCT images and consequently its impact over the dose warped is still a problem to be solved (Qin *et al* 2018, Giacometti *et al* 2020). Furthermore, the combined dosimetric effect of daily periodic respiration and inter-fraction motion in lung SBRT has not yet been investigated (Karlsson *et al* 2021).

The purpose of this study was to estimate the dosimetric impact of two sources of uncertainty in lung SBRT: daily periodic respiratory motion and inter-fraction anatomical variations. We evaluated these sources of uncertainty separately and combined, in three scenarios. Dose calculations were performed in 4D-CT and 4D-CBCT scans and DIR was used to map dose to the planned situation. To account for residual uncertainties, we evaluated the dosimetric results in scenario-specific evaluation target volumes (ETVs) (Azcona *et al* 2019). DIR accuracy was quantified with the Distance Discordance Metric (DDM) (Saleh *et al* 2014, Juan-Cruz *et al* 2021) and a novel 4D method was developed to put the dosimetric impact of DIR inaccuracies in perspective to effects from breathing motion and anatomical changes.

2. Material and methods

2.1. Patient selection

Twenty patients with lung lesions treated with SBRT in three fractions (3×18 Gy or 3×15 Gy) were retrospectively selected for this study following IRB approval. Intentionally, we selected patients with large breathing amplitudes ($\geqslant$1 cm in at least one dimension) to observe the impact of respiration. A 4D-CT scan for

Table 1. Patient characteristics in lung SBRT.
Abbreviations: SD = standard deviation.

Patient characteristics in lung SBRT	
Gender, n *(%)*	
Male	16 (80)
Female	4 (20)
Age	
Mean (SD)	71 (13)
Tumor volume (c.c.)	
Mean (SD)	44 (27.39)
Tumor stage, n *(%)*	
T1	10 (50)
T2	5 (25)
Metastasis	5 (25)
Tumor location, n *(%)*	
Left lower lobe	8 (40)
Right lower lobe	7 (35)
Right middle lobe	3 (15)
Right upper lobe	2 (10)
Peak-to-peak amplitude (cm), mean (SD)	
Left-right	0.17 (0.13)
Cranio-caudal	1.64 (0.60)
Antero-posterior	0.4 (0.15)
Mean vector length	1.7 (0.61)
Safety margins (cm), mean (SD)	
Left-right	0.8 (0)
Cranio-caudal	1.05 (0.15)
Antero-posterior	0.9 (0)
Dose prescription (fractions × *Gy),* n *(%)*	
3 × 18	17 (85)
3 × 15	3 (15)

treatment planning and a daily 4D-CBCT scan immediately prior to treatment were available for each patient. Clinical characteristics are shown in table 1.

2.2. Treatment and image guidance procedure

A free-breathing 4D-CT scan (24-slice Somatom Sensation Open, Siemens, Forchheim, Germany) was acquired for all patients, with a resolution of $0.98 \times 0.98 \times 3\ mm^3$. For 4D-CT, we use time sorting: The respiratory signal was registered using a thermocouple (Wolthaus *et al* 2008) and divided into ten bins of equal duration, giving raise to ten time-sorted datasets. A mid-position 3D-CT (Wolthaus *et al* 2008), derived from the 4D-CT, served as planning CT (pCT) for delineation of the Gross Tumor Volume (GTV) and organs at risk (OARs) and for plan optimization. The expansion from GTV to the Planning Target Volume (PTV) was obtained using the van Herk margin recipe (Van Herk *et al* 2000) combined with the breathing amplitude from the 4D-CT (Sonke *et al* 2009). The PTV accounts for periodic respiratory motion, intra-fraction drifts during the treatment delivery, delineation uncertainty and residual inter-fraction motion (further details about margins construction are explained in section 2.5). Treatment plan optimization was performed in Pinnacle (version 9.2; Philips Radiation Oncology Systems, Milpitas, CA), using the adaptive convolve as the dose calculation algorithm with a $2 \times 2 \times 2\ mm^3$ of dose grid. In all plans, at least 95% of the PTV received the prescribed dose with a PTV maximum dose constraint of 165% of the prescribed dose. All patients were treated with a dual arc Volumetric Modulated Arc Therapy (VMAT) technique on a linac with an integrated CBCT scanner (Elekta Synergy 4.6; Elekta Oncology Systems Ltd, Crawley, UK), augmented with in-house developed software.

Patients were initially set up to the pCT reference position using tattoos and the room lasers. The image guidance procedure implemented (Rossi *et al* 2016) consisted of two CBCT scans acquired in each fraction: after an initial patient setup, a 4D-CBCT scan for tumor alignment was acquired: the bony anatomy was rigidly registered to the pCT based on a rectangular region of interest around the vertebrae. Then, a local tumor rigid registration to the pCT (translations only) was carried on a shaped region of interest (ROI; GTV + 0.5 cm margin) defined on the pCT. Each bin of the 4D-CBCT was rigidly registered with this ROI, leading to the tumor trajectory relative to the pCT. The time-averaged tumor displacement was calculated to quantify tumor baseline shifts, which were used for setup corrections. A 2nd 4D-CBCT scan ($CBCT_{postcorr}$) was obtained for validation of the tumor alignment. For the 4D-CBCT acquisition, the respiratory signal was extracted from the series of

projection data of the CBCT acquisition (Sonke *et al* 2005). The reconstruction was into ten bins using phase sorting. Then, each CBCT bin will not present exactly the equal time. The voxel size was $2 \times 2 \times 2$ mm^3. Note that only the $CBCT_{postcorr}$ was used for dose calculation and accumulation, as explained below (section 2.4).

2.3. Deformable image registration

Deformable Image Registration (DIR) is an image processing technique that establishes a spatial relation between voxels with the same anatomical point in different sets of images (Brock *et al* 2017). The relation is typically described with Deformation Vector Fields (DVFs). A featured-constrained and intensity-based registration algorithm included in ADMIRE (Han 2010) (v2.0, Elekta AB, Stockholm, Sweden) was used to perform CT-CT and CT-CBCT registrations and generate DVFs to map Hounsfield Units (HUs) and/or dose distributions.

For CT-to-CT DIR, each 4D-CT bin was deformed to the pCT. The DVF was denoted as $\boldsymbol{T_j}$, where j represents the corresponding respiratory bin. Through these $\boldsymbol{T_j}$, the dose distributions calculated on each bin j were mapped to the pCT using trilinear interpolation (Chetty and Rosu-Bubulac 2019). This DIR approach has been validated using the DDM concept (Saleh *et al* 2014) (see section 2.6), which has shown to be a reliable predictor of DIR precision (Juan-Cruz *et al* 2021).

In the second situation we mapped CT-to-CBCT. In this case, we used the DVF for both HU propagation to the CBCT and dose mapping back to the pCT. To this end, the pCT was deformed to each daily 4D-CBCT bin. The DVF was denoted as $\boldsymbol{R_{ij}}$, where i is the daily fraction and j refers to each bin of the 4D-CBCT. $\boldsymbol{R_{ij}}$ was used to map the HUs from pCT to each daily 4D-CBCT to create virtual CTs (vCTs) (Giacometti *et al* 2018, 2020) for dose calculation. In this process, the tissue density was assumed constant (validation of vCT creation is provided in *supplementary material* - section 1). Due to the limited CBCT field of view (Giacometti *et al* 2018, 2020), each 4D-CBCT bin was patched (after a rigid registration) with the corresponding 4D-CT bin before DIR. For dose mapping, the inverse of $\boldsymbol{R_{ij}}$ was determined to map the dose onto the pCT by using trilinear interpolation (Chetty and Rosu-Bubulac 2019). The geometric validation of these $\boldsymbol{R_{ij}}$ was quantified by calculating the DDM, which was used to perform a workflow to determine its dosimetric impact (see section 2.6).

2.4. Dosimetric impact of daily respiration and anatomical variations

Three scenarios were evaluated to quantify the separate and combined effect of respiratory motion and daily anatomical variations on the dose distribution: (1) respiratory motion alone, (2) daily anatomical variation alone, (3) respiratory motion and daily anatomical variation (see figure 1). The three scenarios were compared to the planned dose distribution on the 3D MidP CT scan (pCT), represented as $3D_{Ref}$ (figure 1(A)). Identical dose calculation algorithm and parameters used in the treatment plan optimization were used in each scenario.

2.4.1. Effect of baseline respiratory motion

The 4D-CT consists of ten bins over the respiratory cycle and represents the geometrical variations due to respiratory motion. Following a validated method of other groups (Admiraal *et al* 2008, Mexner *et al* 2009, Valdes *et al* 2017, Azcona *et al* 2019) to quantify the effect of respiratory motion (figure 1(B)), the dose was recalculated on these ten bins, subsequently transferred to pCT by $\boldsymbol{T_j}$ and finally accumulated ($4D_{Ref}$). Since the 4D-CT acquisition was divided in bins of equal duration, each transferred dose was weighted by 1/10.

2.4.2. Effect of daily anatomical variations

Daily 4D-CBCT ($CBCT_{postcorr}$) scans were acquired just prior to treatment to capture day-to-day anatomical variations (e.g. posture changes, baseline shifts or anatomy configuration) and variations in respiratory motion. To evaluate only the effect of daily anatomy variations, a daily virtual CT was generated in the mid-position ($CBCT_{MidP}$) (figure 1(C)). For this purpose, the weighted average of all DVFs $\boldsymbol{R_{i1}}$, $\boldsymbol{R_{i2}}$ … $\boldsymbol{R_{i10}}$ was calculated in each fraction i, resulting in $\boldsymbol{M_{Ri}}$. Weighting was applied to account for the difference in time spent in each bin of the 4D-CBCT. These mean DVFs were used to transfer the HUs from pCT to daily mid-position to create a vCT (denoted as $CBCT_{MidP}$) in each fraction. Then, the daily fraction dose was recalculated on each $CBCT_{MidP}$, deformed back to the pCT using the inverse vectors $\boldsymbol{M_{R_i}^{-1}}$ and summed to obtain the total accumulated dose ($3D_{Acc}$). Both methods, creation of a vCT for daily dose calculation (Szeto *et al* 2016, Cole *et al* 2018, Giacometti *et al* 2018, Yuan *et al* 2020) and mapping the daily dose for accumulation (Veiga *et al* 2015, Szeto *et al* 2016, Wang, *et al* 2020), have been previously validated.

2.4.3. Effect of daily anatomical variations including daily respiration

Daily 4D-CBCT scans acquired just prior to treatment ($CBCT_{postcorr}$) were used to evaluate the combined effect of daily respiratory motion along with daily anatomical variations (figure 1(D)). First, the HUs of the pCT were transferred to each bin from the daily 4D-CBCT by $\boldsymbol{R_{ij}}$ resulting in vCTs with the CBCT anatomy in each bin for each fraction. Then, the dose was recalculated on each vCT, mapped back to the pCT (weighted by a factor of k_{ij}

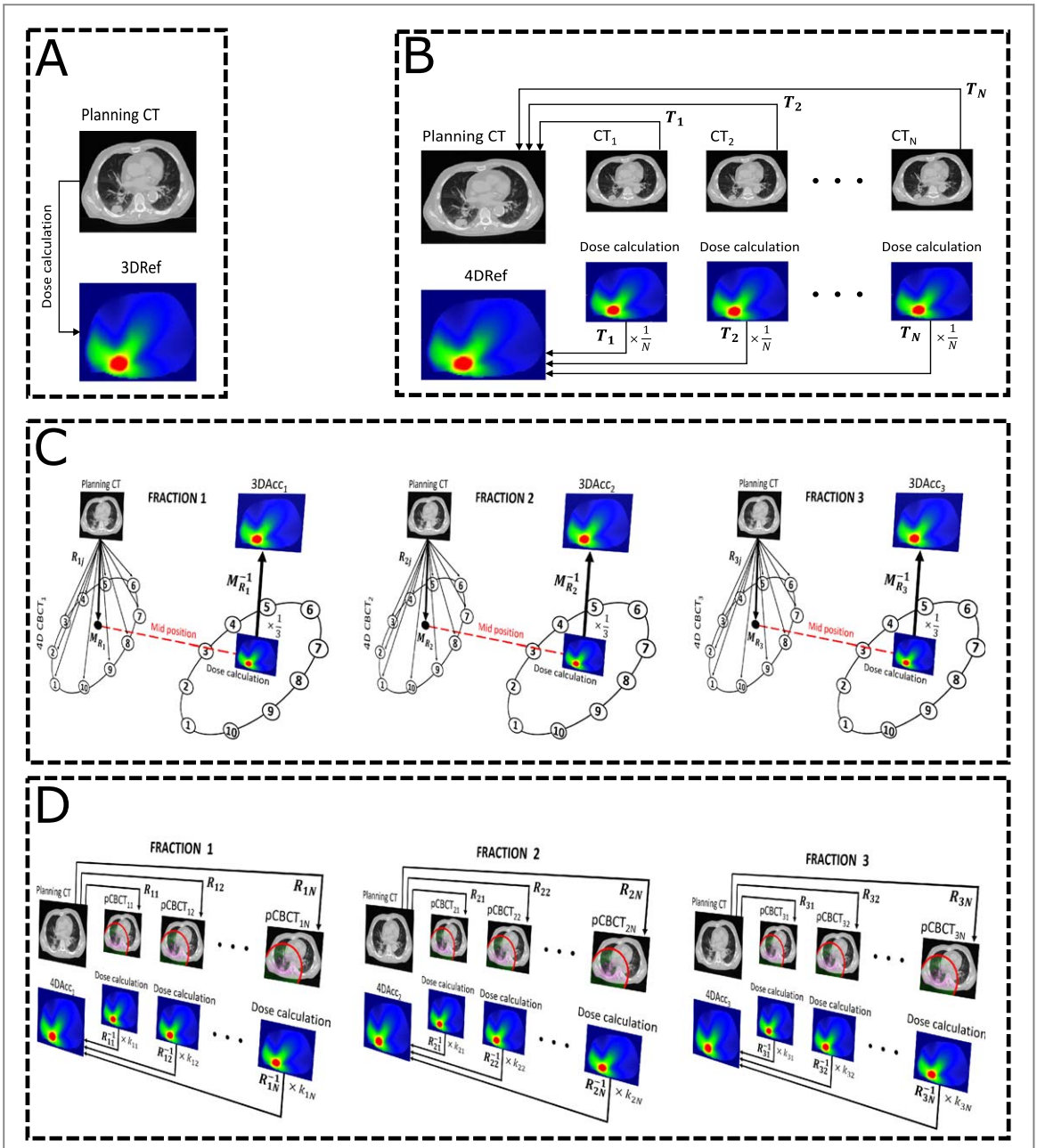

Figure 1. Methodologies implemented to quantify the effect of respiration (panel B), daily anatomical variations (panel C) and both effects combined (panel D) over the treatment planning dose (panel A). Panel D shows the 4D-CBCT patched (after a rigid registration) with the corresponding 4D-CT before the creation of virtual CT (vCT). The red line identifies the CBCT field of view (FOV) and green/purple represent anatomical differences between 4D-CT and 4D-CBCT bins.

to account for the difference in time spend in each bin) by $\boldsymbol{R_{ij}^{-1}}$ and accumulated ($4D_{Acc}$). $4D_{Acc}$ represents the dosimetric impact of daily anatomical variations and respiratory motion during the course of the treatment.

2.5. Dose comparison, margins and dose evaluation

2.5.1. Dose comparison

Dose comparisons were done based on total doses. In this manner, the dose differences between $4D_{Ref}$, $3D_{Acc}$, and $4D_{Acc}$ with $3D_{Ref}$ were calculated per voxel in a mask that includes voxels $\geqslant$25% of maximum dose in $3D_{Ref}$ within the CBCT field of view, as well as $4D_{Acc}$ with $3D_{Acc}$ (in this case, the mask includes voxels $\geqslant$25% of maximum dose in $3D_{Acc}$).

2.5.2. Margins

To optimize and evaluate the plan ($3D_{Ref}$ situation), the PTV margins were calculated for VMAT-based delivery by using the margin van Herk recipe (Van Herk *et al* 2000) including patient specific respiratory motion (Sonke *et al* 2009). However, to evaluate target coverage in the accumulated doses $4D_{Ref}$, $3D_{Acc}$, and $4D_{Acc}$, the use of the

Table 2. Summary of ETVs construction per scenario. TD: target delineation uncertainty; Loc: localization accuracy; IFM: intra-fraction motion; Resp: periodic respiratory motion.

Scenario	Systematic errors ($\boldsymbol{\Sigma}$)	Random errors ($\boldsymbol{\sigma}$)
$4D_{Ref}$	$\sqrt{\Sigma_{TD}^2 + \Sigma_{Loc}^2 + \Sigma_{IFM}^2}$	$\sqrt{(\sigma_{DIR}^{CT-CT})^2 + \sigma_{Loc}^2 + \sigma_{IFM}^2}$
$3D_{Acc}$	$\sqrt{\Sigma_{TD}^2 + \Sigma_{IFM}^2}$	$\sqrt{(\sigma_{DIR}^{CT-CBCT})^2 + \sigma_{Resp}^2 + \sigma_{IFM}^2}$
$4D_{Acc}$	$\sqrt{\Sigma_{TD}^2 + \Sigma_{IFM}^2}$	$\sqrt{(\sigma_{DIR}^{CT-CBCT})^2 + \sigma_{IFM}^2}$

Table 3. Summary of residual geometric uncertainty components for Planned Target Volume (PTV) and Evaluation Target Volume (ETV) margins construction. LR: left-right direction; CC: cranio-caudal direction; AP: antero-posterior direction; A: breathing amplitude.

Residual geometric uncertainty components	LR (cm)	CC (cm)	AP (cm)
Systematic target delineation error: Σ_{TD}	0.2	0.2	0.2
Systematic localization accuracy error: Σ_{Loc}	0.08	0.08	0.09
Systematic intra-fraction motion error: Σ_{IFM}	0.06	0.06	0.09
Random localization accuracy error: σ_{Loc}	0.11	0.11	0.14
Random intra-fraction error: σ_{IFM}	0.13	0.15	0.18
Random respiratory motion error: σ_{Resp}	$0.36 \cdot A_{LR}$	$0.36 \cdot A_{CC}$	$0.36 \cdot A_{AP}$
Random error for CT-to-CT DIR: σ_{DIR}^{CT-CT}	0.09	0.18	0.10
Random error for CT-to-CBCT DIR: $\sigma_{DIR}^{CT-CBCT}$	0.10	0.26	0.17

PTV is not appropriate because it includes periodic respiratory and inter-fraction motion which were already incorporated in the dose accumulation process. Therefore, the Evaluation Target Volume (ETV) (Azcona *et al* 2019, Huesa-Berral *et al* 2021) was used instead. The ETV is expanded from the GTV (=CTV) and accounts for: (1) DIR geometric uncertainty, (2) the interobserver GTV delineation uncertainty and (3) the intra-fraction motion during treatment delivery. The ETV margin was calculated using the nonlinear van Herk margin recipe (Van Herk *et al* 2000, Sonke *et al* 2009) as follows:

$$M_{ETV} = 2.5\Sigma + 0.84(\sqrt{\sigma^2 + \sigma_p^2} - \sigma_p). \quad (1)$$

With Σ and σ represent the total systematic and random errors, respectively. They were calculated as $\Sigma = \sqrt{\Sigma_{TD}^2 + \Sigma_{Loc}^2 + \Sigma_{IFM}^2}$ and $\sigma = \sqrt{\sigma_{Resp}^2 + \sigma_{Loc}^2 + \sigma_{IFM}^2}$, where the subscript refers to: target delineation (TD), localization accuracy—residual tumor misalignment following IGRT corrections—(Loc), intra-fraction motion during treatment delivery (IFM) and respiration (Resp). Based on this equation, ETV margins were calculated for the prescription isodose line, which is often approximately 80% in lung SBRT (Sonke *et al* 2009), with a width of a single penumbra of $\sigma_p = 6.4$ mm. Nonetheless, the geometric components such as respiration (σ_{Resp}) and location accuracy (Σ_{Loc}, σ_{Loc}) are or not included in equation (1) depending on the scenario evaluated. Table 2 shows a summary of each ETV applied per scenario.

For $4D_{Ref}$ scenario, DIR errors were calculated based on CT-CT DIR validation and for $3D_{Acc}$ and $4D_{Acc}$ scenarios, DIR errors were obtained from CT-CBCT DIR validation (see section 2.6.2., equation (3)). Here we assume that DIR uncertainty can be described by a normal distribution (0, σ_{DIR}) (Brock *et al* 2017).

Quantitative values for the various residual geometric uncertainty components for both PTV and ETV margins were obtained from Sonke *et al* (2009) and are provided in table 3.

2.5.3. Dose evaluation

Dose volume histogram (DVH) parameters were calculated to evaluate tumor coverage and OARs dosage: For PTV and ETVs, D_{95} and D_1 were assessed to evaluate dose prescription consistency. For comparison with literature, the minimum and maximum dose to 99% and 1% of the volume (D_{99} and D_1) were calculated for the GTV. OARs were evaluated on the maximum dose (D_{max}) for ribs, spinal cord, heart and esophagus, the mean dose (D_{mean}) for lung, heart and esophagus and the dose delivered to 5%, 10% and 20% of the volume (V_5, V_{10}, V_{20}) for lung. All these dosimetric indicators were calculated over the four dose distributions obtained: $3D_{Ref.}$, $4D_{Ref}$, $3D_{Acc}$, and $4D_{Acc}$, and the differences with respect to $3D_{Ref}$ were evaluated, as well as differences between $4D_{Acc}$, and $3D_{Acc}$.

2.6. Validation of deformable image registration

Two different DIR techniques were used for dose mapping: CT-CT DIR for the $4D_{Ref}$ scenario and CT-CBCT DIR for the $3D_{Acc}$ and $4D_{Acc}$ scenarios. As a result, two sets of DVFs (one per DIR technique) were generated to map dose into the pCT. The accuracy of the DVFs was validated for both DIR techniques in this section.

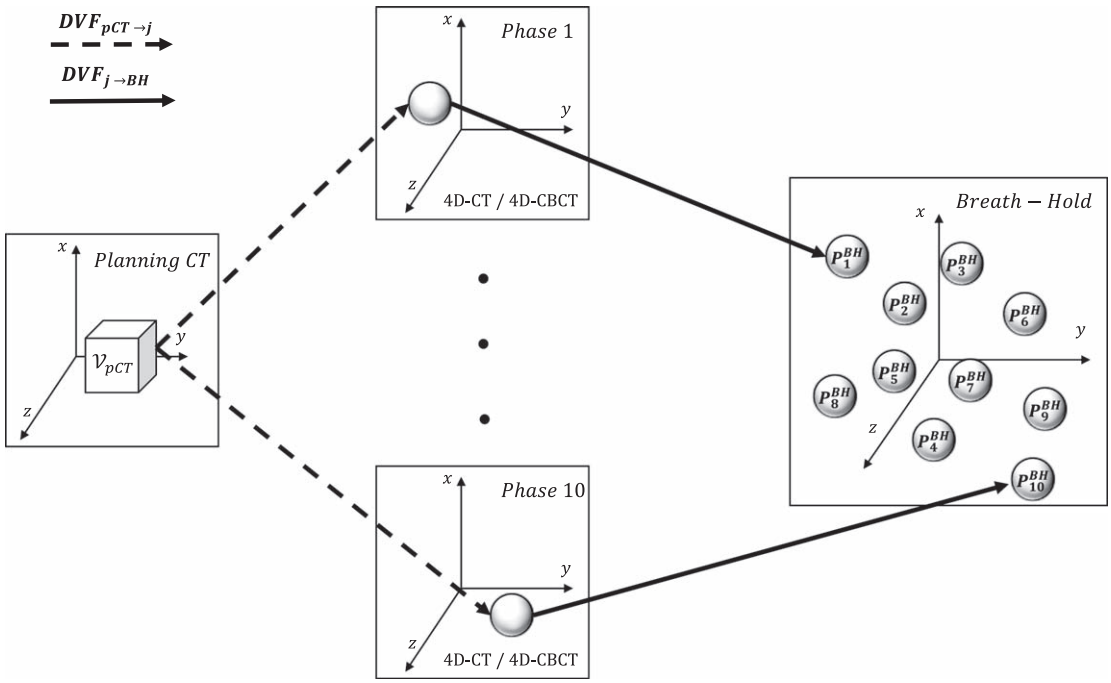

Figure 2. Methodology for DDM definition implemented in this work. A voxel $\mathcal{V}_{pCT}$ is propagated to a specific location in the breath-hold scan for each bin j (P_j^{BH}). Bins can be selected from the 4D-CT or the 4D-CBCT.

Table 4. Peak-to-peak 4D-CT amplitude and 3D tumor baseline shift for the corresponding treatment fraction for ten patients

Independent cohort selected for DIR validation	
Peak-to-peak amplitude (cm), mean (SD)	
Left-right	0.29 (0.15)
Cranio-caudal	2.18 (0.34)
Antero-posterior	0.4 (0.25)
Mean vector length	2.25 (0.32)
Tumor baseline shift (cm), mean (SD)	
Left-right	0.14 (0.07)
Cranio-caudal	0.52 (0.24)
Antero-posterior	0.38 (0.22)
Mean vector length	0.69 (0.24)

2.6.1. Patient selection

An independent cohort of ten patients with lung lesions treated with SBRT in three fractions with large 3D tumor motion were selected to validate the CT-CT and CT-CBCT DIR. Between the three fractions, the one with the highest 3D tumor baseline shift was selected and the 4D-CBCT just prior to treatment was available. For all patients, a 3D MidP planning CT (Wolthaus *et al* 2008), as well as a breath-hold scan at exhale, acquired for planning, was available. This cohort was intentionally selected to represent the challenging cases for DIR. Table 4 shows the tumor motion and the 3D tumor baseline shift for these patients.

2.6.2. Geometric validation: DDM

The geometric validation of CT-to-CT and CT-to-CBCT DIR was done using the DDM (Saleh *et al* 2014), which has shown to be a good predictor of DIR precision (Juan-Cruz *et al* 2021). We used a modified version of the DDM in which we indirectly registered the planning CT to the breath-hold CT via various in between bins (from 4D-CT or 4D-CBCT), see figure 2.

Ten deformations paths were generated between the pCT (initial image) and the breath-hold (BH) scan (end image), through 4D-CT and/or 4D-CBCT bins. The pCT was deformed to each of the ten bins, resulting in one DVF per bin j ($DVF_{pCT \to j}$). Another ten DVFs ($DVF_{j \to BH}$) were generated by the DIR of each bin j to the breath-

hold scan at exhale. Finally, the combination of these DVFs results in a unique DVF per bin *j*: $DVF_{j\to BH} \circ DVF_{pCT\to j}$. Each of these combined DVFs was applied to each voxel $\mathcal{V}$ in the pCT ($\mathcal{V}_{pCT}$), which was propagated to ten different locations (one per bin *j*) in the BH scan (P_j^{BH}). We defined the DDM as the standard deviation over the ten different locations of each propagated voxel, corrected for the number deformations (assuming normally distributed registration errors, treating each direction independently):

$$DDM(\mathcal{V}_{pCT}) = \frac{SD_{x,y,z}(P_{j=1\ldots10}^{BH})}{\sqrt{2}}. \tag{2}$$

For CT-CT modality the bins were those of 4D-CT, and for CT-CBCT the bins were selected from the 4D-CBCT. The 3D vector of $DDM(\mathcal{V}_{pCT})$-denoted as DDM_{3D}—was calculated for each voxel belonging to GTV, lung, ribs, heart, esophagus, and spinal cord. When 4D-CBCT bins were selected, only voxels inside the field of view were evaluated.

This metric is also useful to incorporate the DIR geometric errors within ETV margins for each DIR technique used (table 3, section 2.5.2). In this context, σ_{DIR}^{CT-CT} and $\sigma_{DIR}^{CT-CBCT}$ were calculated following the equation (3):

$$\sigma_{DIR}^{technique} = \sqrt{\frac{\sum_{n=1}^{10} VAR_{GTV_n}[DDM^{technique}]}{10}}, \tag{3}$$

where technique refers to DIR of CT-CT or CT-CBCT, $VAR_{GTV_n}[DDM^{technique}]$ is the variance of the DDM over the voxels of the GTV for patient *n*.

2.6.3. Dosimetric validation: DDM into dosimetric uncertainty

To determine whether the impact of DIR geometric uncertainties is relevant or not, its dosimetric consequence was quantified. To this end, the dose mapping method was applied for the patients collected in table 4 considering DIR geometric errors through DDM computed previously for all of them. We repeatedly mapped the recalculated dose to the reference anatomy, each time introducing an error in the DVF, in agreement with the DDM. The dosimetric impact of CT-CT DIR geometric uncertainties has been previously quantified across ten 4D-CT studies where it was reasonably small (Vickress *et al* 2017), but the dosimetric impact of CT-CBCT DIR (deforming pCT to 4D-CBCT) has not been reported in the literature (Giacometti *et al* 2020). Therefore, the dosimetric impact of DIR was only assessed for the CT-CBCT DIR technique, based on $4D_{Acc}$ scenario.

The methodology steps are presented in figure 3: Per bin, per voxel, a random error *m* ($Error_m$) is sampled from the distribution $N(0,\ DDM(\mathcal{V}_{pCT}))$, and added to the deformation vectors prior to mapping the dose to the pCT, resulting in an accumulated error dose distribution $4D_{Acc}^{Error_m}$. This process was repeated 1000 times, yielding 1000 accumulated error dose distributions. Finally, with a confidence interval width of 95%, the dosimetric impact of DIR is defined per voxel as follows:

$$CIW_{95\%} = \frac{SD(4D_{Acc}^{m=1\ldots1000})}{\sqrt{3}} \times 1.96. \tag{4}$$

3. Results

3.1. Dose comparison

As shown in figure 4, we found little dosimetric effect from respiratory motion. The Interquartile Range (IQR) and the median voxel dose differences (scenario 1, $4D_{Ref} - 3D_{Ref}$) were 0.78 Gy and −0.16 Gy respectively. In contrast, for $3D_{Acc} - 3D_{Ref}$ (scenario 2, the impact of daily anatomical variations) and $4D_{Acc} - 3D_{Ref}$ (scenario 3, the impact of daily respiratory motion and anatomical variations) the IQR and median voxel dose differences were 2.69 Gy, 0.05 Gy and 2.68 Gy, −0.12 Gy, respectively. In fact, scenarios 2 and 3 were very similar, as can be seen from a direct comparison between $4D_{Acc}$ and $3D_{Acc}$: IQR and median were 0.37 Gy and −0.08 Gy respectively.

3.2. Tumor coverage

ETV margins were substantially smaller than PTV margins (*supplementary material,* table S2). Regarding PTV and ETVs, the relevant dose differences were found in ΔD_{95}, where the median was close to 3 Gy for all three scenarios (figures 5(A)–(C)), whereas the ΔD_1 difference was small for all of them. Respiratory motion evaluation (figure 5(A)) showed two patients where D_{95} for ETV was lower than D_{95} for PTV, although the difference (ΔD_{95}) was small: −0.5 and −1 Gy respectively. In the daily anatomical variations evaluation (figure 5(B)) and in the combined effect of respiration and inter-fraction motion assessment (figure 5(C)) only

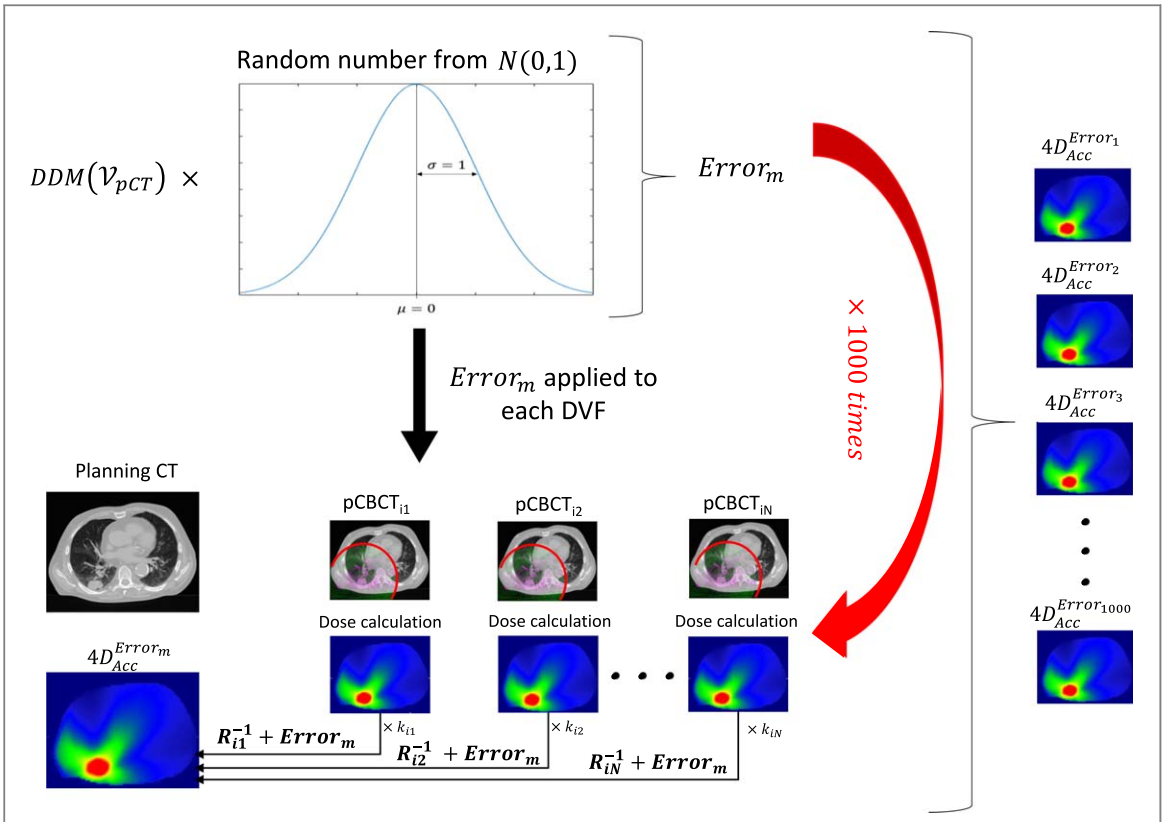

Figure 3. Quantifying the dosimetric impact of DIR geometric uncertainties using DDM. The method was repeated 1000 times to calculate 1000 accumulated error dose distributions $4D_{Acc}$. The standard deviation of these 1000 doses determines the dosimetric impact (equation (4)). The red line identifies the CBCT field of view (FOV) and green/purple represent anatomical differences between 4D-CT and 4D-CBCT bins.

one patient had a negative ΔD_{95}, which was −4 Gy and −3 Gy, respectively. Dose differences ΔD_{95} and ΔD_1 were very small in comparison to $3D_{Acc}$ and $4D_{Acc}$ (figure 5(D)).

For GTV, the median for ΔD_{99} and ΔD_1 was close to 0 Gy, with a IQR below 1.6 Gy in all three scenarios (figures 5(A)–(C)). Dose differences ΔD_{99} and ΔD_1 were negligible for the comparison between $3D_{Acc}$ and $4D_{Acc}$ (figure 5(D)).

3.3. Organs at risk

The dosimetric effect of respiratory motion for the OARs was small, with median and IQR below 0.8 Gy for all differences in DVH parameters, (figure 5(A)). These differences increased when daily anatomical variations were included (figures 5(B), (C)). The largest differences were found in lung (ΔV_5 of 4.18%) and in esophagus (ΔD_{max} of −3.2 Gy) for scenario 3 (figure 3(C)) and in ribs (ΔD_{max} of −3.1 Gy) for scenario 2 (figure 5(B)). Consequently, there were minimal differences for dosimetric indicators when comparing $3D_{Acc}$ and $4D_{Acc}$.

3.4. DIR validation

The results are shown in figure 6: the geometric validation is shown in panels (a) and (b), whereas panel (c) represents the dosimetric impact of DIR errors in CT-CBCT technique. For geometric validation, equation (2) was applied per voxel and per patient in each anatomical structure, showing that the median and 75th percentile was below 2 mm (voxel size) for all anatomical volumes, except for the heart in CT-CT DIR (75th percentile = 3.84 mm, median = 2.62 mm). The 95th percentiles for both DIR applications are displayed in table 5, where CT-CBCT modality showed higher percentiles, mostly in ribs and spinal cord (95th percentiles of 5.13 and 8.00 mm). In general, 95th percentiles for both modalities were around 2 mm.

Regarding the dosimetric impact of those errors for CT-CBCT DIR technique, we obtained $CIW_{95\%}$ by applying equation (4) per voxel and per patient into the GTV and OARs. The violin plots in figure 6 show a comparison between geometric uncertainty (panel (b)) and its dosimetric impact (panel (c)). The dosimetric impact was small for all anatomical structures: the median was close to 0 in all cases, and the 95th percentile was below 1.7 Gy in all anatomical volumes (table 5).

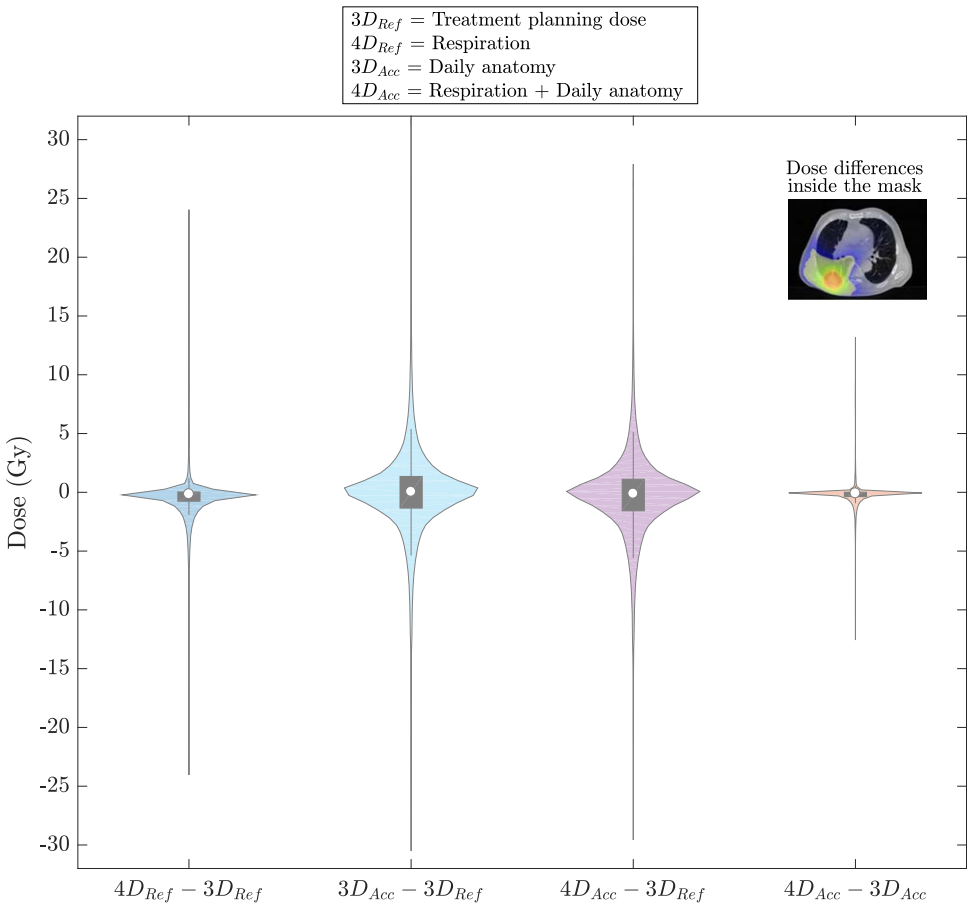

Figure 4. Violin plots (together with the interquartile range and median) of the dose differences per voxel calculated in a mask within the CBCT field of view per each scenario.

4. Discussion

In this study, we provide a detailed analysis and extensive validation of the separate and combined dosimetric effect of periodic respiratory motion and daily anatomical variations in SBRT of pulmonary lesions for a cohort of twenty patients. Our findings demonstrate that inter-fraction anatomical variations have a larger impact on the dose distribution than periodic respiratory motion, therefore 3D Mid-position CBCT based dose accumulation is sufficient for treatment evaluation. Moreover, we demonstrated a novel and systematic method to incorporate 4D DIR uncertainty in dosimetric impact quantification, which was used to validate the three scenarios implemented in this work. Lastly, we found that the combined effect of periodic respiration and daily anatomical variations was smaller than the linear combination of the individual components.

Daily deviations in patient anatomy generally had a larger dosimetric impact than daily periodic respiratory motion for lung SBRT. This can be explained by the nature of both sources of geometric uncertainty. Periodic respiratory motion around the MidP represents a random error and predominantly leads to a blurring of the dose distribution (Bortfeld *et al* 2004). Daily anatomical variations on the other hand represent both random and systematic errors, the latter of which causes a shift of the dose distribution which has a bigger impact than blurring (Sonke *et al* 2019). Moreover, in SBRT delivered dose over a limited number of fractions, the day-to-day random errors may not fully blur-out. Note that we have selected patients with large amplitudes and the majority of patients have a smaller amplitude. Therefore, the dosimetric impact of periodic respiratory motion in a more representative group would likely be even smaller. These observations imply that to estimate the delivered dose it may suffice to only account for daily anatomical changes (figure 1(C)) ignoring periodic respiratory motion. Moreover, it can be concluded that to further improve SBRT delivery robustness, online adaptive strategies accounting for daily anatomical variations may be more effective than active respiratory motion management strategies such as gating.

Concerning DIR accuracy, its validation is necessary for confidence in the dose accumulation methods (Samavati *et al* 2016). In this study, DIR for both modalities were extensively validated. Deforming pCT to 4D-CT (CT-CT DIR modality, the first scenario, figure 1(B)) for dose mapping and accumulation was validated in

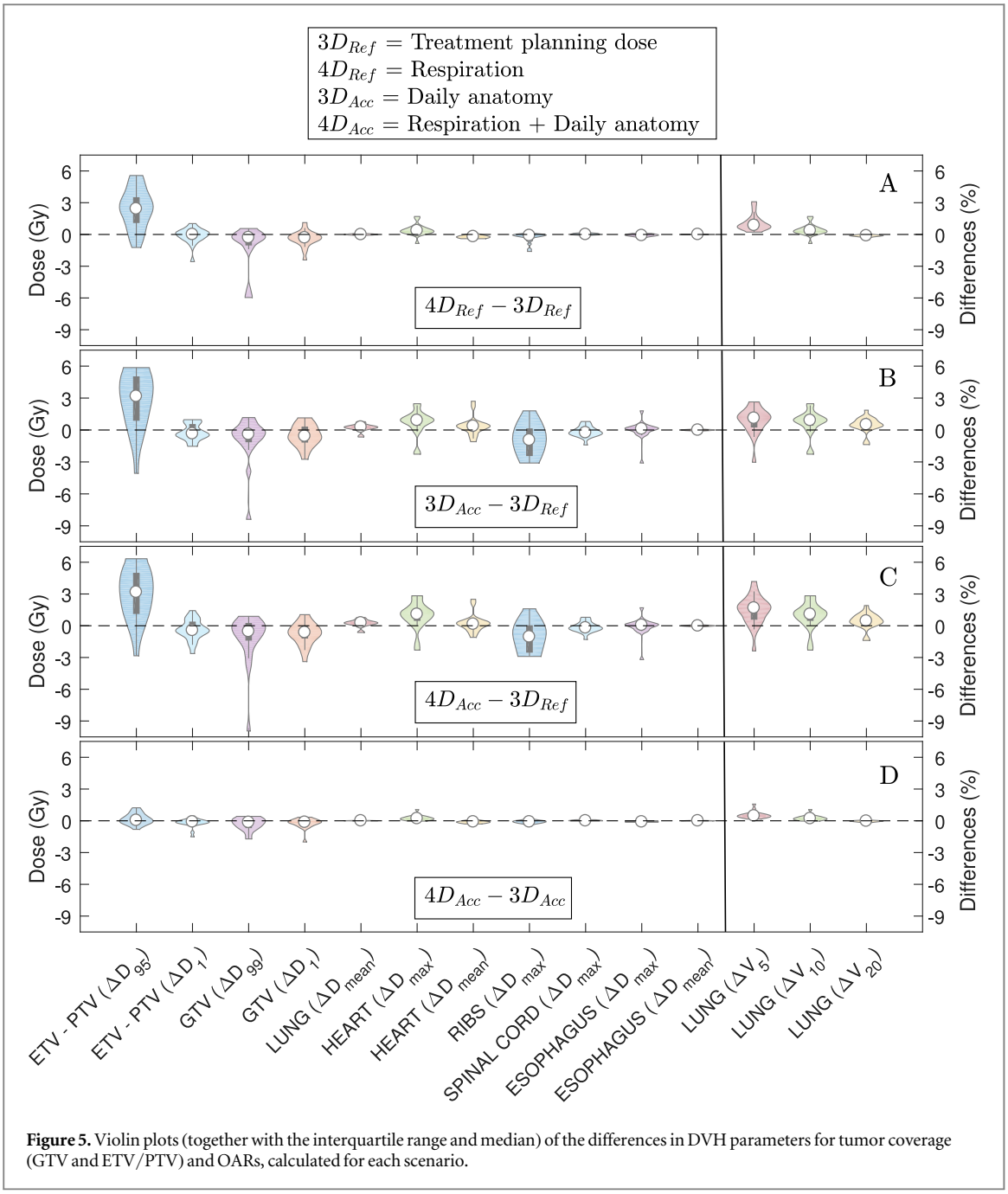

Figure 5. Violin plots (together with the interquartile range and median) of the differences in DVH parameters for tumor coverage (GTV and ETV/PTV) and OARs, calculated for each scenario.

previous studies (Admiraal *et al* 2008, Mexner *et al* 2009, Valdes *et al* 2017, Azcona *et al* 2019). Its accuracy was validated in this study by using a modified version of the DDM (Saleh *et al* 2014). The highest geometric uncertainty was found in heart, due to the discrepancy between heart motion and respiratory motion during 4D-CT acquisition, since 4D-CT is based on the respiratory cycle and not the cardiac cycle. Therefore, substantial artefacts in the heart reconstruction may exist between respiratory bins, possibly leading to larger deformations. The dosimetric impact of this DIR technique was studied previously (Vickress *et al* 2017) and the range of dose uncertainty found to be in the order of 2.5 Gy. For CT-CBCT DIR (second and third scenarios, figures 1(C) and (D)), DDM for heart had smaller values due to acquisition speed: CBCT is slow, and the reconstruction of bins will blur out cardiac bins, and thus lead to less erratic deformations. Here, the anatomical structures with the highest geometric uncertainty were the spinal cord and ribs because of poor CBCT image quality to identify both anatomical structures. Moreover, ribs and spinal cord extends beyond the FOV. However, the dosimetric consequences evaluated in tumor and OARs were small, since the largest impact was observed for GTV, lung and ribs with a 95th percentile dosimetric uncertainty of 1.7, 0.86 and 1.05 Gy respectively. Dose errors from DIR inaccuracies will manifest themselves only at dose gradients. For this reason, although DDM reported for spinal cord in CT-CBCT DIR was 8.00 mm, the dosimetric impact in absence of dose gradients is negligible (*see also*

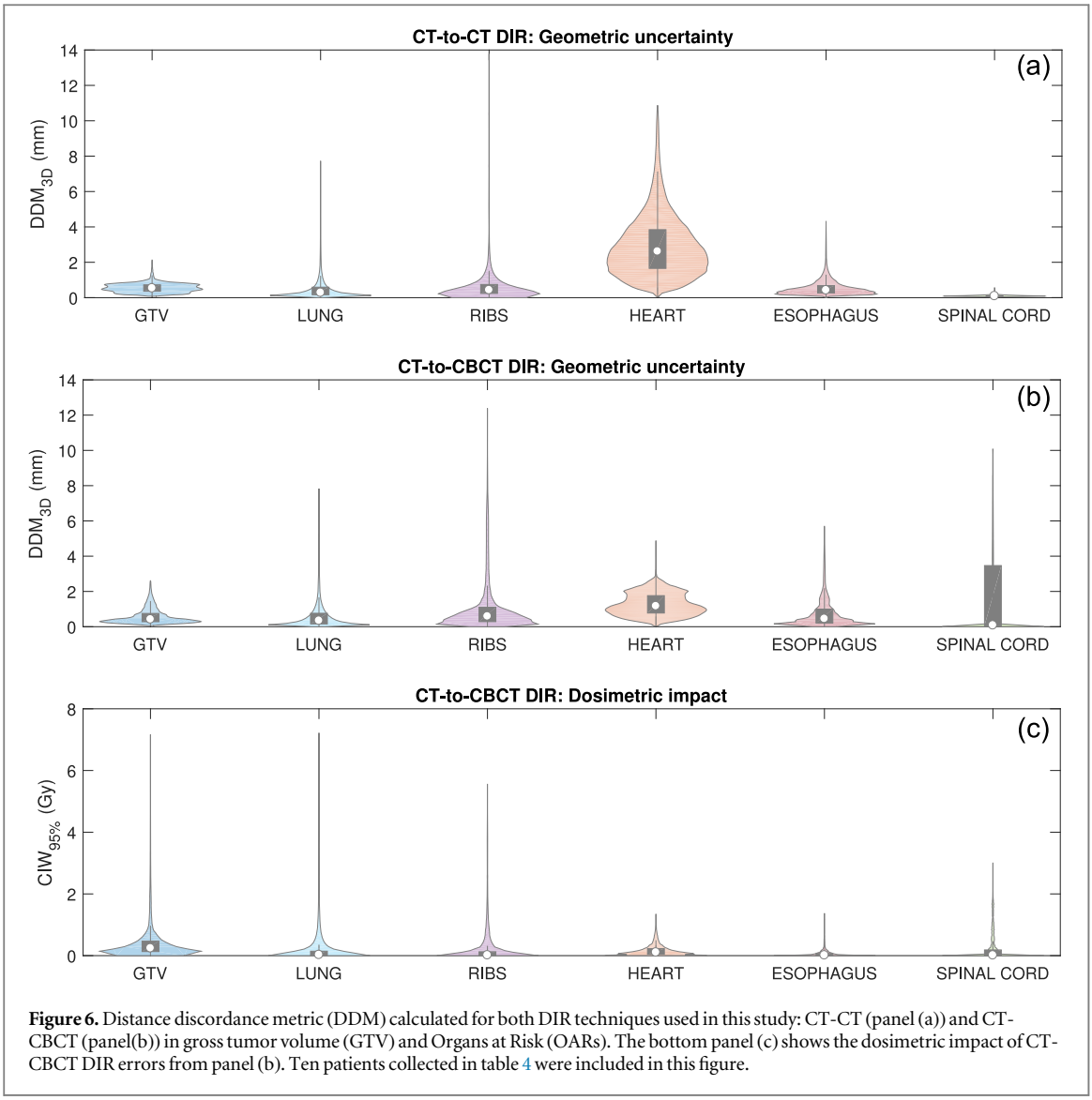

Figure 6. Distance discordance metric (DDM) calculated for both DIR techniques used in this study: CT-CT (panel (a)) and CT-CBCT (panel(b)) in gross tumor volume (GTV) and Organs at Risk (OARs). The bottom panel (c) shows the dosimetric impact of CT-CBCT DIR errors from panel (b). Ten patients collected in table 4 were included in this figure.

Table 5. 95th percentile comparison of distance discordance metric calculated in tumor and organs at risk (OARs) for CT-CT and CT-CBCT DIR techniques (first and second column). The third column shows the 95th percentile about the dosimetric impact of CT-CBCT DIR errors (second column).

Tumor and organs at risk	P_{95}^{CT-CT} (mm)	$P_{95}^{CT-CBCT}$ (mm)	$P_{95}^{CT-CBCT}$ (Gy)
GTV	0.93	1.54	1.67
LUNG	1.86	2.16	0.86
RIBS	1.66	5.13	1.05
HEART	6.26	2.34	0.57
ESOPHAGUS	1.38	2.55	0.29
SPINAL CORD	0.16	8.00	1.28

supplementary material - figure S6). Our DDM based dosimetric impact analysis may be applied on individual patients and could thus be of clinical value.

Regarding the virtual CT (vCT) creation for dose calculation, we propose to map HUs from pCT to 4D-CBCT, although another option could be to map HUs from 4D-CT to 4D-CBCT between the corresponding respiratory bins. We have compared both workflows in terms of dose differences and gamma index and they were small (*supplementary material - section 1.1*). Therefore, we recommend using the pCT for simplicity. In this process, we disregard the conservation of tissue densities, as its effect in dose calculation was negligible (*supplementary material - section 1.2*).

This study investigated the separate and combined dosimetric effect of periodic respiratory motion and daily anatomical variations. It was shown that the combined effect ($4D_{Acc}$) was considerably smaller than the linear combination of the individual components ($4D_{Ref}$ and $3D_{Acc}$). This is consistent with the root-sum-square combination of sources of geometric uncertainties employed in the van Herk margin recipe (Van Herk *et al* 2000).

Target coverage was evaluated by comparing the D_{95} of the PTV and ETV in the planned and accumulated dose distribution respectively. For a robust assessment, the ETV concept (Azcona *et al* 2019, Huesa-Berral *et al* 2021) was integrated in this study adapting their margins to each scenario, including the corresponding DIR technique geometric uncertainty quantified by calculating the DDM. As expected, the median ETV D_{95} was higher than the median PTV D_{95} as the margins were designed to provide target coverage for 90% of the patients. In other words, they are 'too large' for the majority of patients. ETV D_{95} was larger than PTV D_{95} for $\geqslant$90% of patients for all 3 scenario's indicating that the plans were sufficiently robust against periodic respiratory motion and daily anatomical variations for tumor coverage. Only one patient had a considerably lower accumulated ETV D_{95} than planned (-3 and -4 Gy, figures 5(B), (C)), as well as for GTV D_{99} (-6 and -9 Gy, figures 5(A)–(C)). The reason was that the tumor was close to an OAR (main bronchus) and a baseline shift towards this critical structure was observed. Therefore, a residual tumor misalignment was accepted during the IGRT procedure to prevent OAR overdosing.

The PTV margins in this study were based on the MidP concept instead of the more widely used Internal Target Volume (ITV) approach. The ITV approach uses larger margins for periodic respiratory motion while ITV-to-PTV margins are often smaller ignoring e.g. delineation variation. Performing our study in a population treated with an ITV approach would likely confirm our finding that the dosimetric impact of periodic respiration is smaller than those daily anatomical variations. In case of small respiratory motion and corresponding ITVs (in 1 or more directions) such study may also find more underdosage of the ETV than observed in this study.

An important component of the ETV in this study was a target delineation uncertainty of 0.2 cm. This estimate was based on a target delineation variability study on 4D CT derived mid-ventilation scans (Peulen *et al* 2015) In case of 3D CT scans, the target shape may be distorted due to artifacts associated with the interplay of respiratory motion and CT imaging (Vedam *et al* 2003, Ford *et al* 2003). Therefore, careful management of respiratory motion during treatment preparation to facilitate accurate target definition remains an important component of 4D-CBCT guided SBRT.

The dosimetric impact of daily anatomical changes and periodic respiratory motion for OARs were typically smaller than for the target. For SBRT of peripheral pulmonary lesions, most OARs are relatively far away and outside high dose gradients. Consequently, geometrical uncertainties will have limited dosimetric impact. The lesions are surrounded by the lung but the dosimetric parameters associated with pulmonary toxicity such as the mean lung dose are also quite robust against geometrical uncertainties. The ribs were one of the OARs where the dose differences were highest. Here the difference in the D_{max} over all ribs was reported corresponding to the rib closest to the high dose region. Consequently, the reported D_{max} is more succeptible to geometrical uncertainties. Clinically it was not a concern, as the observed dosimetric differences are likely to have a limited impact on the probability of toxicity (Stam *et al* 2017).

Dose accumulation over the respiratory cycle has been reported in the literature. Our results are in line with other studies published, where their findings revealed that the dosimetric impact of periodic respiration was small in tumor and OARs (Mexner *et al* 2009, Valdes *et al* 2017, Admiraal *et al* 2008, Azcona *et al* 2019). Although dose accumulation for inter-fractions variations over a large number of fractions has been reported (Yuan *et al* 2020, Wang *et al* 2020), in lung SBRT it has not been widely studied. Recently, Karlsson *et al* (2021) estimated the delivered dose to the target simulating inter-fraction and periodic breathing motion errors by dose accumulatios of shifting the static treatment plan dose distribution. They found that errors due to breathing motion had a less impact than setup and IGRT errors, in line with our findings. Nevertheless, as they pointed out, the dose shift-approximation they used is a methodological limitation, since the dose-follows-anatomy paradigm in lung RT may significantly alter dose distributions. With our work, we overcome that limitation. Furthermore, continuing on the clinical conclusion that inter-fraction motion dominates over periodic respiration, we have developed and validated a method to evaluate unclear cases in clinic.

This study has several limitations. We assumed that both 4D-CT and 4D-CBCT amplitudes are constant andrepresentative of breathing motion. Steiner *et al* (2019) on the other hand, pointed out that both techniques under-predict lung target motion range. Since the impact of breathing motion is characterized by its standard deviation rather than its range and plays a secondary role compared to inter-fraction motion (Rit *et al* 2012), we do not expect a significant impact of the observation of Steiner *et al*. Furthermore, we ignored intra-fraction drifts during beam delivery. However, we do not expect an impact on the dose distribution larger than respiration and/or daily anatomical variations: intra-fraction motion was previously analyzed in a large population revealing small tumor drifts during treatment delivery (below 2 mm -voxel size- per axis in both

systematic and random errors) (Rossi *et al* 2016). Indeed, they quantified a reduction below 0.3 mm in safety margins when intra-fraction drifts were minimized by approximately 30%. Another limitation in this study is the limited number of patients included from a single institution. Moreover, we disregarded the interplay effect between the movement of the multileaf collimator and respiratory motion in dynamic treatments techniques (Bortfeld *et al* 2004), although previous studies showed the interplay effect to be negligible for tumor and OARs (Huesa-Berral *et al* 2021, Edvardsson *et al* 2018). Furthermore, dose mapping in this study was based on trilinear interpolation (Chetty and Rosu-Bubulac 2019), basically ignoring energy per mass conservation. While for periodic motion and for short-course RT treatments, where substantial tissue changes are not likely, energy conservation should be assumed, we expect little effect. However, further studies detailing the effects of energy per mass transfer mapping should be considered (Li *et al* 2014, Siebers and Zhong 2008).

5. Conclusion

The dosimetric impact of daily anatomical variations are larger than those of periodic respiratory motion in SBRT for pulmonary lesions. Therefore, treatment evaluation and dose-effect studies would benefit more from dose accumulation focusing on day-to-day changes than those that focus on respiratory motion. In this context, the extensively validated methodology we provide based on dose accumulation over the daily 3D Mid-position CBCT is sufficient for treatment assessment. Similarly, adaptive radiotherapy strategies to mitigate the impact of daily anatomical variations are likely more effective than respiratory motion management strategies.

Acknowledgments

Carlos Huesa-Berral and Juan Diego Azcona acknowledge the financial support from the Spanish Secretary of Economy and Competitiveness through the Health Institute Carlos III (project PI16/00899) and the European Regional Development Fund (ERDF). Carlos Huesa-Berral also acknowledges the fellowships from the Friend Association of the University of Navarra and from the Navarra Government. Jan-Jakob Sonke acknowledges grants from Elekta Oncology Systems AB outside the submitted work.

The authors thank Lennert Ploeger, Georgios Sotiropoulos and Igor Olaciregui for software assistance.

Ethical statement

This retrospective study was approved by the Institutional review board (IRB) of the Netherlands Cancer Institute\Antoni van Leeuwenhoek hospital with approval number IRBd20-008.

ORCID iDs

Carlos Huesa-Berral https://orcid.org/0000-0003-2290-0176
Juan Diego Azcona https://orcid.org/0000-0001-7242-4169
Jan-Jakob Sonke https://orcid.org/0000-0001-5155-5274

References

Admiraal M A, Schuring D and Hurkmans C W 2008 Dose calculations accounting for breathing motion in stereotactic lung radiotherapy based on 4D-CT and the internal target volume *Radiother. Oncol.* **86** 55–60

Azcona J D, Huesa-Berral C, Moreno-Jiménez M, Barbés B, Aristu J J and Burguete J 2019 A novel concept to include uncertainties in the evaluation of stereotactic body radiation therapy after 4D dose accumulation using deformable image registration *Med. Phys.* **46** 4346–55

Bortfeld T, Jiang S B and Rietzel E 2004 Effects of motion on the total dose distribution *Semin. Radiat. Oncol.* **14** 41–51

Brock K K, Mutic S, Mc Nutt T R, Li H and Kessler M L 2017 Use of image registration and fusion algorithms and techniques in radiotherapy: report of the aapm radiation therapy committee task group no. 132 *Med. Phys.* **44** 43–76

Brown S *et al* 2021 The impact of intra-thoracic anatomical changes upon the delivery of lung stereotactic ablative radiotherapy *Clin. Oncol. (R. Coll. Radiol.)* **14** S0936–6555

Chetty I J and Rosu-Bubulac Mihaela 2019 : Deformable registration for dose accumulation *Semin. Radiat. Oncol.* **29** 198–208

Cole A J, Veiga C, Johnson U, D'Souza D, Lalli N K and McClelland J 2018 Toward adaptive radiotherapy for lung patients: Feasibility study on deforming planning CT to CBCT to assess the impact of anatomical changes on dosimetry *Phys. Med. Biol.* **63** 155014

Edvardsson A, Nordström F, Ceberg C and Ceberg S 2018 Motion induced interplay effects for VMAT radiotherapy *Phys. Med. Biol.* **19** 085012

Ehrbar S, Jöhl A, Tartas A, Stark L S, Riesterer O, Klöck S, Guckenberger M and Tanadini-Lang S I T V 2017 mid-ventilation, gating or couch tracking—a comparison of respiratory motion-management techniques based on 4D dose calculations *Radiother. Oncol.* **124** 80–8

Ford E C, Mageras G S, Yorke E and Ling C C 2003 Respiration-correlated spiral CT: a method of measuring respiratory-induced anatomic motion for radiation treatment planning *Med. Phys.* **30** 88–97

Giacometti V et al 2018 An evaluation of techniques for dose calculation on cone beam computed tomography Br. J. Radiol. 92 1–11
Giacometti V, Hounsell A R and McGarry C K 2020 A review of dose calculation approaches with cone beam CT in photon and proton therapy Phys. Med. 76 243–76
Han X 2010 Feature-constrained nonlinear registration of Lung CT images Med. Image Anal. Clin.: Grand Challenge 63–72 (https://docplayer.net/49683603-Feature-constrained-nonlinear-registration-of-lung-ct-images.html)
Huesa-Berral C, Burguete J, Moreno-Jiménez M and Azcona J D 2021 A method using 4D dose accumulation to quantify the interplay effect in lung stereotactic body radiation therapy Phys. Med. Biol. 66 035025
Jaffray D A, Siewerdsen J H, Wong J W and Martinez A A 2002 Flat-panel cone-beam computed tomography for image-guided radiation therapy Int. J. Radiat. Oncol. Biol. Phys. 53 1337–49
Juan-Cruz C, Fast M F and Sonke J J 2021 A multivariable study of deformable image registration evaluation metrics in 4DCT of thoracic cancer patients Phys. Med. Biol. 2021 66 035019
Karlsson K, Lax I, Lindbäck E, Grozman V, Lindberg K, Wersäll P and Poludniowski G 2021 Estimation of delivered dose to lung tumours considering setup uncertainties and breathing motion in a cohort of patients treated with stereotactic body radiation therapy Phys. Med. 88 53–64
Keall P J et al 2021 AAPM Task Group 264: the safe clinical implementation of MLC tracking in radiotherapy Med. Phys. 48 e44–64
Li H S, Zhong H, Kim J, Glide-Hurst C, Gulam M, Nurushev T S and Chetty I J 2014 Direct dose mapping versus energy/mass transfer mapping for 4D dose accumulation: fundamental differences and dosimetric consequences Phys. Med. Biol. 6 173–88
Mexner V, Wolthaus J W H, van Herk M, Damen E M F and Sonke J J 2009 Effects of respiration-induced density variations on dose distributions in radiotherapyof lung cancer Int. J. Radiat. Oncol. Biol. Phys. 74 1266–75
Peulen H, Belderbos J, Guckenberger M, Hope A, Grills I, van Herk M and Sonke J J 2015 Target delineation variability and corresponding margins of peripheral early stage NSCLC treated with stereotactic body radiotherapy Radiother. Oncol. 114 361–6
Qin A et al 2018 A clinical 3D/4D CBCT-based treatment dose monitoring system J. Appl. Clin. Med. Phys. 19 166–76
Rit S, van Herk M, Zijp L and Sonke J J 2012 Quantification of the variability of diaphragm motion and implications for treatment margin construction Int. J. Radiat. Oncol. Biol. Phys. 82 e399–407
Rossi M, Peulen H, Belderbos J and Sonke J J 2016 Intrafraction motion in stereotactic body radiation therapy for non-small cell lung cancer: Intensity modulated radiation therapy versus volumetric modulated arc therapy Int. J. Radiat. Oncol. Biol. Phys. 95 835–43
Saleh Z H et al 2014 The distance discordance metric-a novel approach to quantifying spatial uncertainties in intra- and inter-patient deformable image registration Phys. Med. Biol. 59 733–46
Samavati N, Velec M and Brock K K 2016 Effect of deformable registration uncertainty on lung SBRT dose accumulation Med. Phys. 43 233
Schwarz M, Cattaneo G M and Marrazzo L 2017 Geometrical and dosimetrical uncertainties in hypofractionated radiotherapy of the lung: a review Phys. Med. 36 126–39
Siebers J V and Zhong H 2008 An energy transfer method for 4D Monte Carlo dose calculation Med. Phys. 35 4096–105
Sonke J J et al 2009 Frameless stereotactic body radiotherapy for lung cancer using four-dimensional cone beam CT guidance Int. J. Radiat. Oncol. Biol. Phys. 74 567–74
Sonke J J, Aznar M and Rasch C 2019 Adaptive radiotherapy for anatomical changes Semin. Radiat. Oncol. 29 245–57
Sonke J J and Belderbos J 2010 Adaptive radiotherapy for lung cancer Semin. Radiat. Oncol. 20 94–106
Sonke J J, Zijp L, Remeijer P and Van Herk M 2005 Respiratory correlated cone beam CT Med. Phys. 32 1176–86
Stam B, van der Bijl E, Peulen H, Rossi M M, Belderbos J S and Sonke J J 2017 Dose–effect analysis of radiation induced rib fractures after thoracic SBRT Radiother. Oncol. 123 176–81
Steiner E et al 2019 Both four-dimensional computed tomography and four-dimensional cone beam computed tomography under-predict lung target motion during radiotherapy Radiother. Oncol. 135 65–73
Szeto Y Z, Witte M G, van Kranen S R, Sonke J J, Belderbos J and van Herk M 2016 Effects of anatomical changes on pencil beam scanning proton plans in locally advanced NSCLC patients Radiother. Oncol. 120 286–92
Valdes G et al 2017 The relative accuracy of 4D dose accumulation for lung radiotherapy using rigid dose projection versus dose recalculation on every breathing phase Med. Phys. 44 1120–7
Van Herk M et al 2000 The probability of correct target dosage: Dose-population histograms for deriving treatment margins in radiotherapy Int. J. Radiat. Oncol. 47 1121–35
Van Herk M 2004 Errors and margins in radiotherapy Semin. Radiat. Oncol. 14 52–64
Van Herk M 2007 Different styles of image-guided radiotherapy Semin. Radiat. Oncol. 17 258–67
Vedam S S, Keall P J, Kini V R, Mostafavi H, Shukla H P and Mohan R 2003 Acquiring a four-dimensional computed tomography dataset using an external respiratory signal Phys. Med. Biol. 48 45–62
Veiga C et al 2015 Toward adaptive radiotherapy for head and neck patients: Uncertainties in dose warping due to the choice of deformable registration algorithm Med. Phys. 42 760–69
Vickress J, Battista J, Barnett R and Yartsev S 2017 Representing the dosimetric impact of deformable image registration errors Phys. Med. Biol. 62 N391–403
Wang B et al 2020 Accumulation of the delivered dose based on cone-beam CT and deformable image registration for non-small cell lung cancer treated with hypofractionated radiotherapy BMC Cancer 16 112
Wolthaus J W, Sonke J J, van Herk M, Belderbos J S, Rossi M M, Lebesque J V and Damen E M 2008 Comparison of different strategies to use four-dimensional computed tomography in treatment planning for lung cancer patients Int. J. Radiat. Oncol. Biol. Phys. 70 1229–38
Wolthaus J W H, Schneider C, Sonke J J and Damen E M F 2008 Reconstruction of a time-averaged midposition CT scan for radiotherapy planning of lung cancer patients using deformable registration Med. Phys. 35 3998–4011
Yang M and Timmerman R 2018 Stereotactic ablative radiotherapy uncertainties: delineation, setup and motion Semin. Radiat. Oncol. 28 207–17
Yuan Z, Rong Y, Benedict S H, Daly M E, Qiu J and Yamamoto T 2020 'Dose of the day' based on cone beam computed tomography and deformable image registration for lung cancer radiotherapy J. Appl. Clin. Med. Phys. 21 88–94